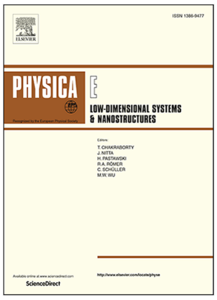

Electronic, optical and photocatalytic properties of fully hydrogenated GeC monolayer

Tuan V. Vu, Nguyen Thi Tuyet Anh, D.M. Hoat, Duy Phu Tran, Hien D. Tong, Hai L. Luong, Le Minh Hieu, Chuong V. Nguyen, Huynh V. Phuc, Nguyen T.T. Binh, Nguyen N. Hieu

PII: S1386-9477(19)31620-0
DOI: https://doi.org/10.1016/j.physe.2019.113857
Reference: PHYSE 113857

To appear in: *Physica E: Low-dimensional Systems and Nanostructures*

Received date : 24 October 2019
Revised date : 26 November 2019
Accepted date : 27 November 2019

Please cite this article as: T.V. Vu, N.T.T. Anh, D.M. Hoat et al., Electronic, optical and photocatalytic properties of fully hydrogenated GeC monolayer, *Physica E: Low-dimensional Systems and Nanostructures* (2019), doi: https://doi.org/10.1016/j.physe.2019.113857.

Electronic, optical and photocatalytic properties of fully hydrogenated GeC monolayer

Tuan V. Vu [a,b], Nguyen Thi Tuyet Anh [c], D. M. Hoat [d], Duy Phu Tran [e], Hien D. Tong [f], Hai L. Luong [g], Le Minh Hieu [h], Chuong V. Nguyen [i], Huynh V. Phuc [j], Nguyen T.T. Binh [k,*], Nguyen N. Hieu [k]

[a]*Division of Computational Physics, Institute for Computational Science, Ton Duc Thang University, Ho Chi Minh City, Viet Nam*

[b]*Faculty of Electrical & Electronics Engineering, Ton Duc Thang University, Ho Chi Minh City, Viet Nam*

[c]*Department of Physics, University of Education, Hue University, Hue, Viet Nam*

[d]*Computational Optics Research Group, Advanced Institute of Materials Science, Ton Duc Thang University, Ho Chi Minh City, Viet Nam*

[e]*Future Industries Institute, University of South Australia, Mawson Lakes, Campus Mawson Lakes, South Australia 5095, Australia*

[f]*Faculty of Engineering, Vietnamese-German University, Binh Duong, Viet Nam*

[g]*Department of Physics, Ho Chi Minh City University of Education, Ho Chi Minh City, Viet Nam*

[h]*Department of Economics, University of Economics, The University of Danang, 71 Ngu Hanh Son Street, Da Nang 550000, Viet Nam*

[i]*Department of Materials Science & Engineering, Le Quy Don Technical University, Ha Noi, Viet Nam*

Preprint submitted to Elsevier *26 November 2019*

[j]*Division of Theoretical Physics, Dong Thap University, Cao Lanh, Viet Nam*

[k]*Institute of Research and Development, Duy Tan University, Da Nang 550000, Viet Nam*

Abstract

In this work, we study the electronic, optical, and photocatalytic properties of fully hydrogenated GeC monolayer under strain engineering and external electric field using first-principles investigations. Our calculations demonstrate that at the equilibrium state, fully hydrogenated GeC monolayer is a indirect-semiconductor with band gap of 3.493 eV and it possesses photocatalytic characteristics for water splitting and in particular, photocatalytic activities can be enhanced by a negative electric field under ultraviolet light. We can control the band gap of fully hydrogenated GeC monolayer by biaxial strain or external electric field and semiconductor–metal phase transition happens at certain elongation of biaxial strain. Compared to pure monolayer GeC, the fully hydrogenation causes optical absorption peaks of GeC shifting to a higher energy region. While the optical spectra of the fully hydrogenated GeC monolayer are strongly dependent on the strain, the effect of the electric field on them is negligible. Our findings can provide useful information for the applicability of fully hydrogenated GeC monolayer in nanoelectronic devices and photocatalytic water splitting.

Key words: Monolayer germanium carbide, fully hydrogenation, electronic and optical properties, photocatalytic water splitting, first-principles calculations

---

[*] Corresponding author.
Email addresses: `vuvantuan@tdtu.edu.vn` (Tuan V. Vu), `nguyentthanhbinh8@duytan.edu.vn` (Nguyen T.T. Binh), `hieunn@duytan.edu.vn` (Nguyen N. Hieu).

1 Introduction

Since graphene was discovered in 2004 by Novoselov and co-workers [1], it has become one of the hottest materials for a long time due to its outstanding physical and chemical properties [2]. The success of graphene in applications in nanotechnoloies has created a wide-ranging search for two-dimensional graphene-like materials in the scientific community [3–7]. Besides graphene, other two-dimensional materials, such as phosphorene [8], dichalcogenides [9,10] or monochalcogenides [11–13], have shown many outstanding physical properties that can be applied in nanoelectronic devices. Recently, it has been shown that MoS_2 [14], blue phase GeS and GeSe monolayers [15], and hydrogenated boron–carbon monolayer [16], which are as efficient photocatalyst, has many promising applications for water splitting. Hydrogenation of monolayers has been able to bring many new properties, which are not in pure materials [16–19].

Pure GeC is a semiconductor with a honeycomb structure similar to graphene [17]. In monolayer form, GeC belongs to $P\bar{6}m2$ symmetry group. Previous density functional theory (DFT) calculations showed that band gap of GeC depends strongly on its thickness (i.e., number of layers) [20] and one can control the band gap of layered GeC via strain engineering [20] or external electric field [21]. While planar honeycomb structure of Ge is unstable [22], the planar honeycomb structure of GeC compound is stable [23]. Şahin and co-workers [23] have indicated that GeC monolayer has high in-plane stiffness, up to 142 J/m^2. This value is quite higher than that of other compounds such as SnGe (35 J/m^2), SiGe (57 J/m^2) or SnC (98 J/m^2) [23].

To search of new properties of materials, one of the methods of recent interest is a surface functionalization [24]. Drissi and co-workers have investigated the different fluorinated GeC configurations using DFT calculations [25]. One have shown that the hydrogenation on the different atom sites of semi-hydrogenated SiC monolayer led to change its electronic and magnetic properties [19]. Besides, the hydrogenation can control the phase transition in transition metal dichalcogenides [26]. In the present study, we focus on the electronic, optical and photocatalytic properties of fully hydrogenated GeC monolayer (H–GeC–H). Using DFT calculations, we investigate the influence of biaxial strain and external electric field on physical properties of H–GeC–H. Based on the obtained results, the applicability of fully hydrogenated H–GeC–H in nanoelectronic devices and photocatalytic water splitting applications has also been discussed in this work.

2 Computational method

All calculations of the present work were performed based on DFT using the Quantum Espresso package [27]. The exchange correlation functional was expressed by generalized gradient approximation (GGA) of the Perdew-Burke-Ernzerhof (PBE) functional [28, 29] and a semi-empirical DFT-D2 method by Grimme [30] was used to consider correctly the weak van der Waals interactions which exist in material. The projector augmented-wave method was used to treat the ion-electron interaction. The energy cut-off of 500 eV is used for plane-wave basis. The Brillouin zone is sampled by a $(15 \times 15 \times 1)$ k-mesh for simulations of electronic properties of monolayers GeC and H–GeC–H. All geometry structures in this work were fully relaxed with the criteria for force and energy convergence is respectively 10^{-3} eV/Å and 10^{-6} eV. To eliminate interactions between neighbor slabs, we used a vacuum space of 20 Å along a vertical direction of the monolayer surface.

Table 1

Lattice constants a, Ge–C bond length $d_{\text{Ge–C}}$, C–H bond length $d_{\text{C–H}}$, and Ge–H bond length $d_{\text{Ge–H}}$ (in Å), Δh buckling constant (in Å) and band gaps (in eV) of monolayer GeC and H–GeC–H.

	a	$d_{\text{Ge–C}}$	$d_{\text{C–H}}$	$d_{\text{Ge–H}}$	Δh	Band gap
GeC	3.254	1.879	-	-	-	2.097
H–GeC–H	3.253	1.978	1.106	1.555	0.621	3.493

3 Results and discussion

3.1 Electronic properties of fully hydrogenated germanium carbide H–GeC–H

Monolayer GeC consists of two types of elements of Ge and C in the honeycomb lattice with planar structure. Upon full hydrogenation, the planer structure of GeC becomes a low-bucked structure. Optimized atomic structures of monolayer GeC and fully hydrogenated GeC (H–GeC–H) are depicted in Fig. 1. The optimized lattice constants of monolayers GeC and H–GeC–H are so close, 3.254 Å and 3.253 Å, respectively. However, fully hydrogenation led to a low-bucked structure in GeC with a buckling constant $\Delta h = 0.621$ Å as shown in Fig. 1(e). Besides, the Ge–C bond lengths in the two configurations of unhydrogenated GeC and fully hydrogenzated H–GeC–H also change significantly. The structural parameters of monolayers GeC and H–GeC–H are listed in Tab. 1. Our calculated results for structural parameters of pure and fully hydrogenated GeC are good in agreement with the previous DFT calculations [17]

To start, we first test the dynamically stability of monolayers GeC and H–GeC–H via calculations of their phonon spectra. Phonon dispersion curves of monolayers GeC and H–GeC–H are shown in Fig. 2. Figures 2(a,b) demonstrated that there are no negative frequencies in the phonon spectra of monolayers unhydro-

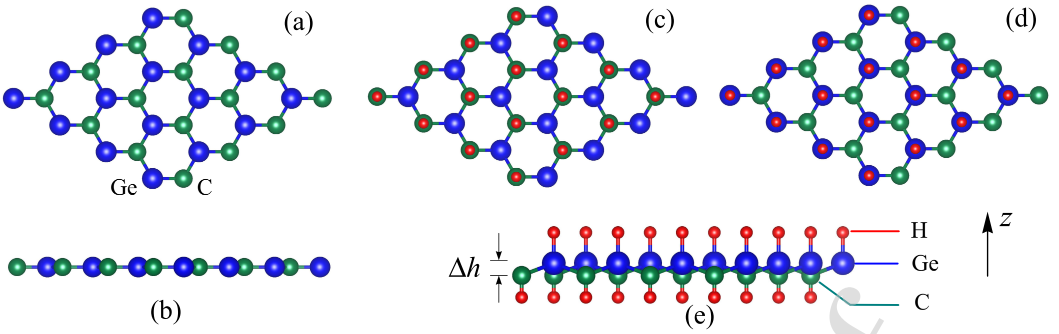

Fig. 1. Optimized atomic structure of monolayers GeC (a,b) and H–GeC–H (c–e).

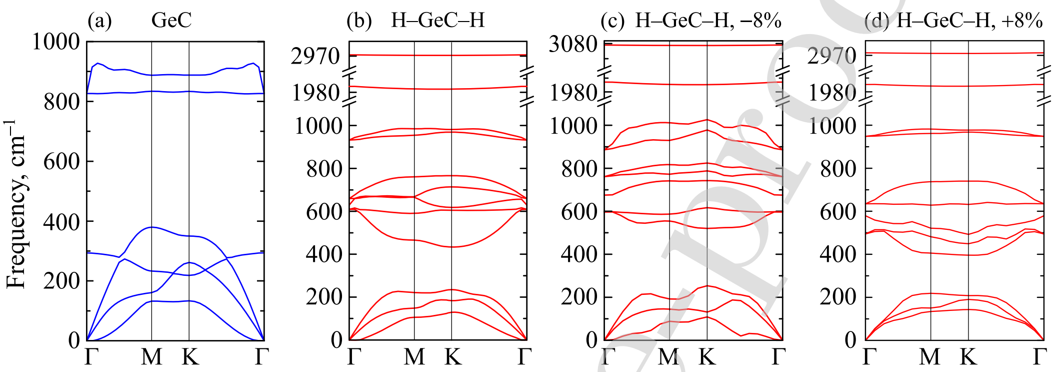

Fig. 2. Phonon spectra of monolayers (a) GeC, (b) H–GeC–H at equilibrium, (c) H–GeC–H at $\varepsilon_b = -8\%$, and (d) H–GeC–H at $\varepsilon_b = 8\%$.

genated GeC and fully hydrogenated H–GeC–H at equilibrium. This implies that, at the equilibrium state, monolayers unhydrogenated GeC and fully hydrogenated H–GeC–H are dynamically stable. Also, we calculate the phonon spectra of the fully hydrogenated H–GeC–H under biaxial strain ε_b as shown in Figs. 2(c,d). The obtained results demonstrate that the fully hydrogenated H–GeC–H is dynamically stable in the presence of biaxial strain from -8% to 8%. Our obtained results indicate that, monolayer unhydrogenated GeC at equilibrium is a direct semiconductor with band gap being 2.097 eV as shown in Fig. 3(a). This result is close to previous DFT calculations by Erasan and co-workers (2.1 eV for GeC) [7]. We see that, upon full hydrogenation, the band gap of monolayer germanium carbide has increased its energy gap by 60%, from 2.097 eV to 3.493 eV as depicted in Fig. 3(b). We show also our DFT calculations for a partial density of states (PDOS) of monolayers

GeC and H–GeC–H at the equilibrium state in Fig. 3. The band structures of the monolayers are calculated along high symmetry direction Γ–M–K–Γ. As shown in Fig. 3(a), monolayer GeC at equilibrium is a direct semiconductor with both the conduction band minimum (CBM) and the valence band maximum (VBM) locating at the K point. Focusing on the PDOS, we can see that the Ge-p and C-$p$orbitals of Ge and C atoms have a significant contribution to the electronic bands of monolayer GeC. In addition, the contribution of the C-$p$orbitals to the valence band is quite larger than that to the conduction band. Besides, the contribution of the Ge-s to the conduction band is also significant. When the GeC is fully hydrogenated, its band structure is significantly changed. Band structure and PDOS of monolayer H–GeC–H are depicted in Fig. 3(b). It is clear to see that, unlike the monolayer GeC, H–GeC–H is a direct semiconductor with a the VBM and CBM locating at the Γ point. Fully hydrogenation not only increases the energy gap of monolayer germanium carbide GeC but also changes the positions of the VBM and CBM in the first Brillouin zone. Due to the fully hydrogenation, both the VBM and CBM are shifted from the K-point to the Γ-point. Focusing on the PDOS of the monolayer H–GeC–H we can see that, along with the contributions of the s- and p-orbitals of the Ge and C atoms, the contribution of the H-s orbital to the electronic bands is significant, in particular, the contribution of the H-s orbital to the valence band in the energy region from -2.2 eV to -3 eV is quite large.

We next investigate the electronic properties of the monolayer H–GeC–H under a biaxial strain ε_b. In this part, we focus on the effect of biaxial strain ε_b on band structure and band gap of the monolayer H–GeC–H in the strain range ε_b from -8% to 8%. Compared to unstrained case, biaxial strain ε_b does not change the position of the CBM and VBM. As a result, in the strain range from -8% to 8%, there is no direct–indirect gap transition in the monolayer H–GeC–H, its band gap is formed from the CBM and the VBM located at the Γ point. However, electronic

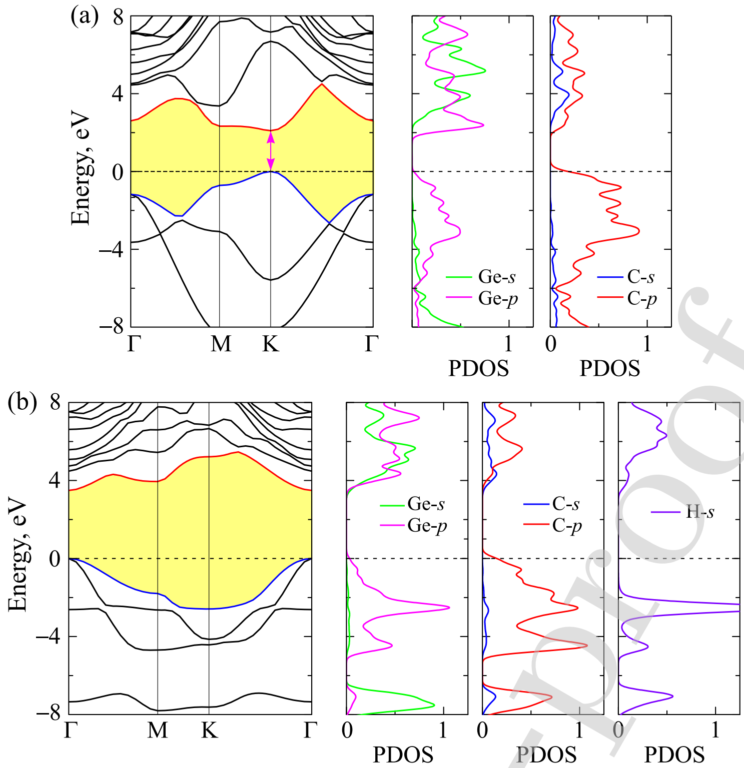

Fig. 3. Band structure of monolayer GeC (a) and H–GeC–H (b) at equilibrium.

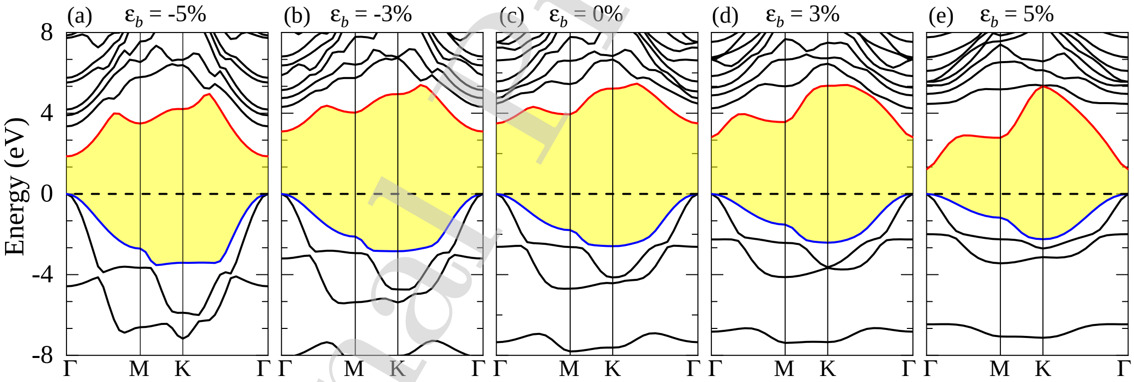

Fig. 4. Band structure and partial density of states (PDOS) of monolayer H–GeC–H under different levels of biaxial strain ε_b: (a) $\varepsilon_b = -5\%$, (b) $\varepsilon_b = -3\%$, (c) $\varepsilon_b = 0\%$, (d) $\varepsilon_b = 3\%$, and (e) $\varepsilon_b = 5\%$

bands, especially the conduction band, of the H–GeC–H depends strongly on the ε_b. While the highest subband of the valence band is less affected by strain engineering and the VBM is always at the Fermi level, the lowest subband of the conduction band changes dramatically with biaxial strain ε_b. The effect of the ε_b on the band

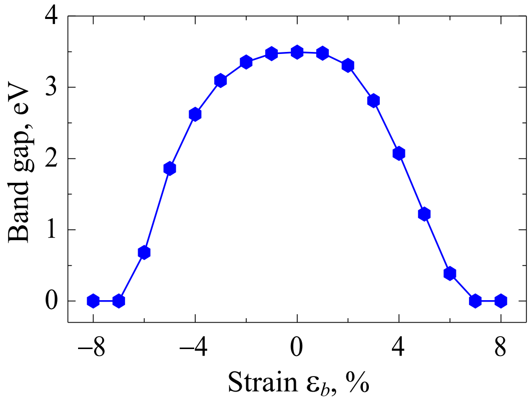

Fig. 5. Dependence of band gap of monolayer H–GeC–H on the ε_b.

structure of monolayer H–GeC–H is shown in Fig. 4. The change of the band gap of monolayer H–GeC–H is mainly due to the conduction band change. Our DFT calculations demonstrate that biaxial strain ε_b reduces the band gap of monolayer H–GeC–H in both cases of tensile and compressive strains. The band gap of monolayer H–GeC–H is maximum at $\varepsilon_b = 0$ (at equilibrium). Dependence of band gap of monolayer H–GeC–H on the ε_b is shown in Fig. 5. We first focus on the tensile case ($\varepsilon_b > 0$). We can see that, in the small range of the ε_b from 0 to 3%, the band gap decreases slowly with strain. However, the band gap decreases quickly as further strain increases. Moreover, the band gap decreases to zero when $\varepsilon_b = 7\%$, meaning that the semiconductor–metal phase transition happens at $\varepsilon_b = 7\%$. The change of band gap in the case of compressive strain is similar to that of tensile strain. The graph which depicts the dependence of band gap on strain ε_b in two cases of the compressive and tensile strains is almost symmetrical across the vertical line passing through the $\varepsilon_b = 0$. It means that the semiconductor–metal phase transition takes place at $\varepsilon_b = \pm 7\%$. Being able to control band gap by strain engineering and the semiconductor–metal phase transition due to strain is a very important indicator for application ability of monolayer H–GeC–H to nanoelectronic devices.

To investigate the influence of an external electric field E on electronic properties of monolayer H–GeC–H, we applied external electric field perpendicular to the

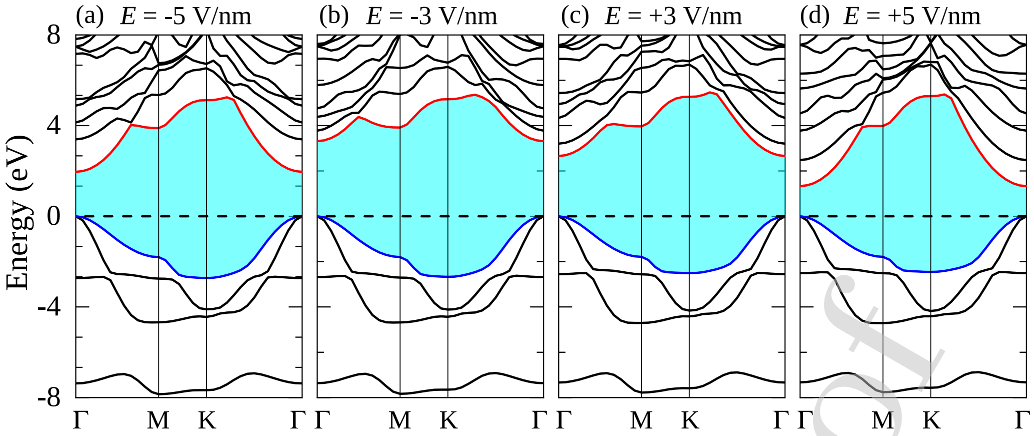

Fig. 6. Band structure of monolayer H–GeC–H under different levels of external electric field E: (a) $E = -5$ V/nm, (b) $E = -3$ V/nm, (c) $E = 3$ V/nm, and (d) $E = 5$ V/nm.

two-dimensional surface of the monolayer. The direction of **E** is along the z-axis. The minus field implies that the **E** is opposite to the z-axis. In presence of the E, electronic properties of monolayer H–GeC–H also change significantly. Figure 6 shows the band structure of monolayer H–GeC–H under external perpendicular electric field E. As shown in Fig. 6, we can see that, similar to under strain engineering, the conduction band of monolayer H–GeC–H depends strongly on the electric field. In the presence of the electric field in the range from -5 V/nm to 5 V/nm, monolayer H–GeC–H is still direct semiconductor. However the band gap monolayer H–GeC–H is extraordinarily dependent on the electric field as shown in Fig. 7. Under the positive electric field (direction of the applied electric field is in the positive direction of the z-axis), the band gap decreases rapidly from 3.493 eV to 1.331 eV when the applied electric field increases from 0 to 5 V/nm. For negative electric field, the band gap of monolayer H–GeC–H increases slightly from 3.493 eV at $E = 0$ V/nm to 3.671 eV at $E = -2$ V/nm and then decreases rapidly when increasing the negative electric field.

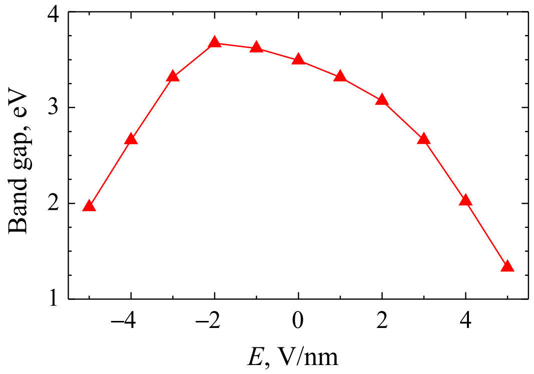

Fig. 7. Band gap of monolayer H–GeC–H as a function of external electric field E.

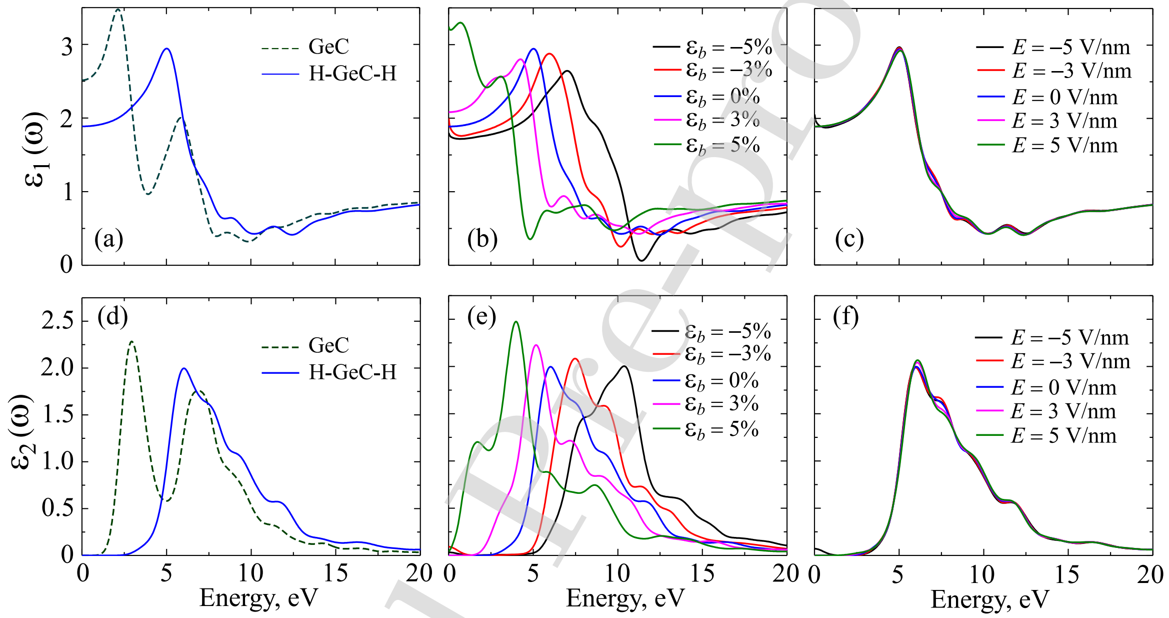

Fig. 8. Real part $\varepsilon_1(\omega)$ and imaginary part $\varepsilon_1(\omega)$ of the dielectric function of monolayer H–GeC–H at equilibrium (a,d) and under biaxial strain ε_b (b,e) and external electric field E (c,f), respectively. The dashed lines in (a) nad (d) are for monolayer GeC.

3.2 Optical properties

In this part, we focus on the influence of the strain engineering ε_b and external electric field E on optical characteristics of monolayer H–GeC–H. We first calculate the dielectric function $\varepsilon(\omega) = \varepsilon_1(\omega) + i\varepsilon_2(\omega)$. Usually, the imaginary part $\varepsilon_2(\omega)$ is calculated first by sum of the occupied–unccupied transitions. Then, we can get the real part $\varepsilon_1(\omega)$ via the Kramer-Kronig transformation [31, 32]. The absorption coefficient $\alpha^{ij}(\omega)$ can be estimated via the parts of dielectric function as $\alpha(\omega) = \frac{\sqrt{2}\omega}{c}\left[\sqrt{\varepsilon_1^2(\omega) + \varepsilon_2^2(\omega)} - \varepsilon_1(\omega)\right]^{1/2}$ [33].

The parts of the dielectric function of monolayer H–GeC–H under biaxial strain ε_b and electric field E are shown in Fig. 8. In Figs. 8(a,d), we show the real $\varepsilon_1(\omega)$ and imaginary $\varepsilon_2(\omega)$ parts of the dielectric function of monolayers GeC and H–GeC–H. We can see that the characteristic peaks of the spectrum of the dielectric function of the monolayer H–GeC–H are similar to those of unhydrogenated GeC. In the monolayer GeC, first peak in $\varepsilon_2(\omega)$ located at 2.94 eV. However, the hydrogenation causes optical absorption peaks of the $\varepsilon_2(\omega)$ in the H–GeC–H to shift to a higher energy region. In the $\varepsilon_2(\omega)$ in the H–GeC–H, first main peaks located at 6 eV. Also, the $\varepsilon_2(\omega)$ part in the H–GeC–H does not respond to the incident light with energy from 0 to 2.5 eV. When the biaxial strain ε_b is applied, the spectra of dielectric function change significantly. While compressive strain causes first peaks of the $\varepsilon(\omega)$ parts in the H–GeC–H to shift to higher energy regions, tensile strain causes them to move to lower energy regions. In particular, at $\varepsilon_b = 5\%$, we see that an additional peak has appeared in the both parts of the $\varepsilon(\omega)$ as shown in Figs. 8(b,e). Figures 8(c,e) indicate that the $\varepsilon_1(\omega)$ and $\varepsilon_2(\omega)$ parts of the dielectric function are almost independent of the external electric field.

In Fig. 9, we show the absorption coefficient $\alpha(\omega)$ of monolayer H–GeC–H in the energy range of the incident light from 0 to 20 eV. Compared to the unhydrogenated case, the maximum absorption coefficient $\alpha(\omega)$ of monolayer H–GeC–H is slightly higher, $\alpha(\omega) = 10.31 \times 10^4$ cm^{-1} at 8 eV. Strain engineering increases significantly absorption coefficient, especially in the compressive case. At $\varepsilon_b = -5\%$, the $\alpha(\omega)$ of monolayer H–GeC–H is up to 15.18×10^4 cm^{-1}. Unlike the dielectric function, the electric field changes the spectrum of the absorption coefficient of monolayer H–GeC–H, however, the absorption coefficient is almost independent of the electric field strength as shown in Fig. 9(c).

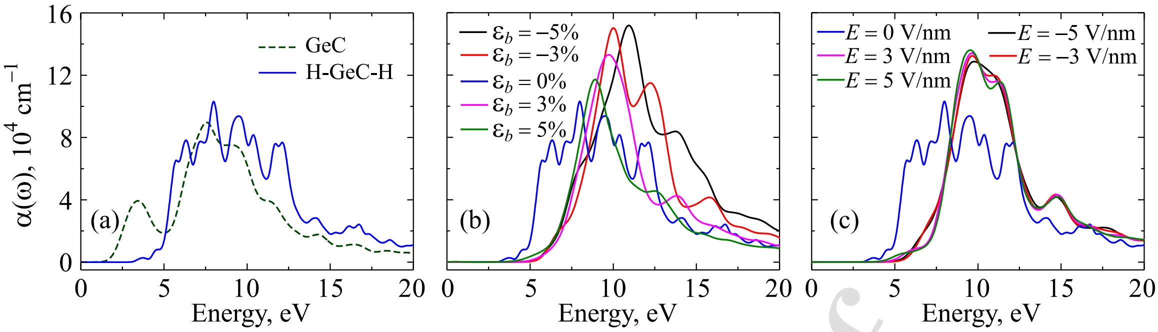

Fig. 9. Absorption coefficient $\alpha(\omega)$ of monolayer H–GeC–H at equilibrium (a) and under biaxial strain ε_b (b) and external electric field E (c). The dashed line in (a) is for monolayer GeC.

3.3 Photocatalytic properties

To find the possible application of monolayer H–GeC–H as a catalyst material for photocatalytic water splitting, we estimate the band edge alignment of monolayer H–GeC–H concerning the redox potentials of the water. We have calculated the CBM and CBM edge alignment of monolayer H–GeC–H under strain and electric field. As shown in Fig. 10, our calculations indicate that the biaxial strain and electric field not only change the band gap but also affect significantly the CBM and CBM edge alignment of monolayer H–GeC–H. The standard oxidation O_2/H_2O and reduction H^+/H_2 potentials for water splitting at $pH = 0$ are respectively $E_{oxi} = -5.67$ eV and $E_{red} = -4.44$ eV [34]. Our calculated results demonstrate that, as shown in Fig. 10, both monolayers GeC and H–GeC–H at equilibrium are suitable for photocatalytic applications. At equilibrium, the CBM is more negative than the reduction potential H^+/H_2 and the VBM is more positive than the standard redox potential of O_2/H_2O. The band gap of monolayer H–GeC–H is 3.493 eV and may decrease due to strain engineering electric field, as analyzed above. It means that the monolayer H–GeC–H under strain or electric field is suitable for an active photocatalyst in the range from ultraviolet to visible light.

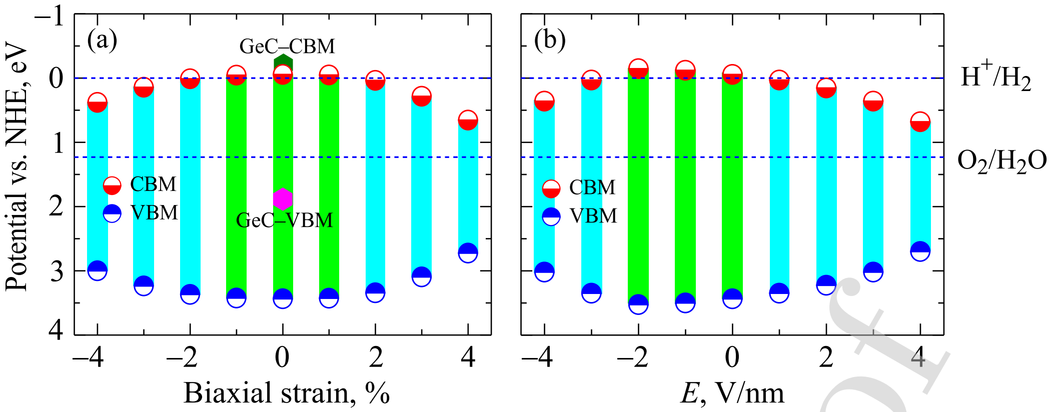

Fig. 10. The CBM and VBM edge alignment of monolayer H–GeC–H in the presence of biaxial strain (a) and electric field E (b). Green and purple hexagons in (a) refer to the CBM and VBM of unhydrogenated GeC at equilibrium, respectively.

In Fig. 10, we can see that the VBM of monolayer H–GeC–H is always located more positive than the standard redox potential of O_2/H_2O when the strain or electric field was introduced. The possible application of monolayer H–GeC–H for photocatalytic water splitting is now dependent on the CBM. When the biaxial strain is applied, the CBM is more negative than the reduction potential H^+/H_2 only in case the ε_b being in the small range of strain from -1% to 1%. In general, strain causes the CBM more positive than the standard redox potential of H^+/H_2. This is not good for the photocatalytic water splitting. When we apply an negative electric field from 0 to -2 V/nm, we can see that the CBM will be located at more negative potential than the standard redox potential of H^+/H_2 as shown in Fig. 10(b). Photocatalytic activity is enhanced within this electric field range.

4 Conclusion

We have systematically studied the electronic, optical and photocatalytic properties of fully hydrogenated GeC monolayer H–GeC–H under biaxial strain and external electric field using first-principles calculations. Compared to pure GeC, the full hydrogenation has increased the band gap of the monolayer H–GeC–H by 60%, from 2.097 eV to 3.493 eV, and caused the optical absorption spectra shifting to a higher energy domain. The electronic properties of a monolayer depend strongly on strain engineering and electric field. In particular, semiconductor–metal phase transitions were found at $\varepsilon_b = \pm 7\%$. While the optical spectra of the monolayer H–GeC–H is almost independent of the external electric field, the strain significantly changes the optical spectra of the monolayer. The absorption coefficient is significantly increased in the presence of strain, especially compressive strain. At equilibrium, the monolayer H–GeC–H possesses photocatalytic properties which is suitable for water photocatalytic splitting applications and we can enhance the photocatalytic activities in monolayer H–GeC–H by the negative electric field.

Acknowledgments

This research is funded by the Vietnam National Foundation for Science and Technology Development (NAFOSTED) under Grant Number 103.01-2018.334.

References

[1] K. S. Novoselov, A. K. Geim, S. V. Morozov, D. Jiang, Y. Zhang, S. V. Dubonos, I. V. Grigorieva, A. A. Firsov, Science 306 (2004) 666.

[2] H. A. Castro Neto, F. Guinea, N. M. R. Peres, K. S. Novoselov, A. K. Geim, Rev. Mod. Phys. 81 (2009) 109.

[3] T. V. Vu, A. Lavrentyev, D. V. Thuan, C. V. Nguyen, O. Khyzhun, B. Gabrelian, K. C. Tran, H. L. Luong, P. D. Tung, K. D. Pham, P. T. Dang, D. D. Vo, Superlattices Microstruct. 125 (2019) 205.

[4] H. R. Jappor, M. M. Obeid, T. V. Vu, D. Hoat, H. D. Bui, N. N. Hieu, S. J. Edrees, Y. Mogulkoc, R. Khenata, Superlattices Microstruct. 130 (2019) 545.

[5] D. Hoat, T. V. Vu, M. M. Obeid, H. R. Jappor, Superlattices Microstruct. 130 (2019) 354.

[6] D. Hoat, T. V. Vu, M. M. Obeid, H. R. Jappor, Chem. Phys. 527 (2019) 110499.

[7] F. Ersan, A. G. Gökce, E. Aktürk, Appl. Surf. Sci. 389 (2016) 1.

[8] P. T. T. Le, K. Mirabbaszadeh, M. Davoudiniya, M. Yarmohammadi, Phys. Chem. Chem. Phys. 20 (2018) 25044.

[9] T. V. Vu, H. D. Tong, T. K. Nguyen, C. V. Nguyen, A. Lavrentyev, O. Khyzhun, B. Gabrelian, H. L. Luong, K. D. Pham, P. T. Dang, D. D. Vo, Chem. Phys. 521 (2019) 5.

[10] C. V. Nguyen, N. N. Hieu, N. A. Poklonski, V. V. Ilyasov, L. Dinh, T. C. Phong, L. V. Tung, H. V. Phuc, Phys. Rev. B 96 (2017) 125411.

[11] P. T. T. Le, C. V. Nguyen, D. V. Thuan, T. V. Vu, V. V. Ilyasov, N. A. Poklonski, H. V. Phuc, I. V. Ershov, G. A. Geguzina, N. V. Hieu, B. D. Hoi, N. X. Cuong, N. N. Hieu, J. Electron. Mater. 48 (5) (2019) 2902.

[12] K. D. Pham, C. V. Nguyen, H. V. Phuc, T. V. Vu, N. V. Hieu, B. D. Hoi, L. C. Nhan, V. Q. Nha, N. N. Hieu, Superlattices Microstruct. 120 (2018) 501.

[13] D. Q. Khoa, C. V. Nguyen, H. V. Phuc, V. V. Ilyasov, T. V. Vu, N. Q. Cuong, B. D. Hoi, D. V. Lu, E. Feddi, M. El-Yadri, M. Farkous, N. N. Hieu, Physica B: Conden. Matter 545 (2018) 255.

[14] Y. Li, Y.-L. Li, C. M. Araujo, W. Luo, R. Ahuja, Catal. Sci. Technol. 3 (2013) 2214.

[15] D. Gu, X. Tao, H. Chen, W. Zhu, Y. Ouyang, Q. Peng, Nanoscale 11 (2019) 2335.

[16] D. Fan, S. Lu, C. Chen, M. Jiang, X. Li, X. Hu, Phys. Chem. Chem. Phys. 21 (2019) 2572.

[17] S. Majidi, N. B. Nezafat, D. P. Rai, A. Achour, H. Ghaziasadi, A. Sheykhian, S. Solaymani, Opt. Quant. Electron. 50 (2018) 292.

[18] X.-Q. Wang, J.-T. Wang, Phys. Lett. A 375 (2011) 2676.

[19] B. Xu, J. Yin, Y. D. Xia, X. G. Wan, Z. G. Liu, Appl. Phys. Lett. 96 (2010) 143111.

[20] Z. Xu, Y. Li, Z. Liu, Mater. Design 108 (2016) 333.

[21] Z. Xu, Y. Li, Z. Liu, C. Li, Physica E 79 (2016) 198.

[22] S. Cahangirov, M. Topsakal, E. Aktürk, H. Şahin, S. Ciraci, Phys. Rev. Lett. 102 (2009) 236804.

[23] H. Şahin, S. Cahangirov, M. Topsakal, E. Bekaroglu, E. Akt''urk, R. T. Senger, S. Ciraci, Phys. Rev. B 80 (2009) 155453.

[24] R. Ruoff, Nat. Nanotechnol. 3 (2008) 10.

[25] L. Drissi, N.-J. Kanga, F. Ramadan, Comput. Conden. Matter 14 (2018) 49.

[26] Y. Qu, H. Pan, C. T. Kwok, Sci. Rep. 6 (2016) 34186.

[27] P. Giannozzi, S. Baroni, N. Bonini, M. Calandra, R. Car, C. Cavazzoni, D. Ceresoli, G. L. Chiarotti, M. Cococcioni, I. Dabo, A. D. Corso, S. de Gironcoli, S. Fabris, G. Fratesi, R. Gebauer, U. Gerstmann, C. Gougoussis, A. Kokalj, M. Lazzeri, L. Martin-Samos, N. Marzari, F. Mauri, R. Mazzarello, S. Paolini, A. Pasquarello, L. Paulatto, C. Sbraccia, S. Scandolo, G. Sclauzero, A. P. Seitsonen, A. Smogunov, P. Umari, R. M. Wentzcovitch, J. Phys.: Condens. Matter 21 (2009) 395502.

[28] J. P. Perdew, K. Burke, M. Ernzerhof, Phys. Rev. Lett. 77 (1996) 3865.

[29] J. P. Perdew, K. Burke, M. Ernzerhof, Phys. Rev. Lett. 78 (1997) 1396.

[30] S. Grimme, J. Comput. Chem. 27 (2006) 1787.

[31] A. Delin, P. Ravindran, O. Eriksson, J. Wills, Int. J. Quantum Chem. 69 (1998) 349.

[32] S. Z. Karazhanov, P. Ravindran, A. Kjekshus, H. Fjellvag, B. G. Svensson, Phys. Rev. B 75 (2007) 155104.

[33] P. Ravindran, A. Delin, B. Johansson, O. Eriksson, J. M. Wills, Phys. Rev. B 59 (1999) 1776.

[34] K. Ren, C. Ren, Y. Luo, Y. Xu, J. Yu, W. Tang, M. Sun, Phys. Chem. Chem. Phys. 21 (2019) 9949.

Highlights

- Fully hydrogenated GeC monolayer is a semiconductor with indirect bandgap of 3.493 eV
- Semiconductor–metal phase transition happens in H-GeC-H at certain elongation of biaxial strain
- Full hydrogenation causes optical absorption peaks of GeC shifting to a higher energy region
- H-GeC-H possesses photocatalytic characteristics for water splitting at equilibrium
- Photocatalytic activities in H-GeC-H can be enhanced by a negative electric field under ultraviolet light

Competing Interests Statement

Manuscript Title:
Electronic, optical and photocatalytic properties of fully hydrogenated GeC monolayer

Authors:
Tuan V. Vu, Nguyen Thi Tuyet Anh, D. M. Hoat, Duy Phu Tran, Hien D. Tong , Hai L. Luong, Le Minh Hieu, Chuong V. Nguyen, Huynh V. Phuc, Nguyen T.T. Binh, Nguyen N. Hieu

On behalf of co-authors

(x) I declare that I have no significant competing financial, professional, or personal interests that might have influenced the performance or presentation of the work described in this manuscript.

Corresponding author

Prof. Nguyen N. Hieu

Duy Tan University, Viet Nam
Email: hieunn@duytan.edu.vn

AUTHORSHIP STATEMENT

Manuscript title: Electronic, optical and photocatalytic properties of fully hydrogenated GeC monolayer

Journal: Physica E: Low-dimensional Systems and Nanostructures

Authors:
Tuan V. Vu, Nguyen Thi Tuyet Anh, D. M. Hoat, Duy Phu Tran, Hien D. Tong , Hai L. Luong, Le Minh Hieu, Chuong V. Nguyen, Huynh V. Phuc, Nguyen T.T. Binh, Nguyen N. Hieu

Authors' contributions

Tuan V. Vu, Nguyen N. Hieu and Nguyen T.T. Binh set the problem of electronic properties of monolayer GeC. Tuan V. Vu, Nguyen Thi Tuyet Anh, D. M Hoat, Duy Phu Tran, Hien D. Tong and Nguyen N. Hieu performed the calculations of the electronic and photocatalytic of fully hydrogenated GeC monolayer. Hai L. Luong , Chuong V. Nguyen and Huynh V. Phuc performed the calculations of the optical properties of the fully hydrogenated GeC monolayer. Tuan V. Vu, Huynh V. Phuc and Nguyen N. Hieu proposed the idea of enhancement of photocatalytic activity of fully hydrogenated GeC monolayer by strain. Chuong V. Nguyen, Tuan V. Vu, Nguyen T.T. Binh and Nguyen N. Hieu contributed to the discussion of effect of strain engineering on the electronic, optical and photocatalytic properties of the fully hydrogenated GeC monolayer and wrote the manuscript. Le Minh Hieu performed the calculations of phonon spectra of the fully hydrogenated GeC monolayer under strain and contributed to revision process of the manuscript.

All authors commented on the manuscript and approved the final manuscript.

On behalf of co-authors

Corresponding author

Prof. Nguyen N. Hieu
Duy Tan University
Viet Nam